Electronic Supplementary Information

Uncommon thioether modified metal-organic frameworks with unique selective CO_2 sorption and efficient catalytic conversion

Wen-Juan Wang, Jiao Liu, Yang-Tian Yan, Xiao-Li Yang, Wen-Yan Zhang*, Guo-Ping Yang*, and Yao-Yu Wang

Key Laboratory of Synthetic and Natural Functional Molecule of the Ministry of Education, Shaanxi Key Laboratory of Physico-Inorganic Chemistry, College of and Materials Science, Northwest University, Xi'an 710127, P.R. China.

Contents

Experimental section

Measurement. The reagents and solvents were purchased without purification in the experiments. Elemental analyses (C, H, N) were tested on Perkin-Elmer 2400 C elemental analyzer. Infrared spectra were tested on Bruker EQUINOX-55 spectrophotometer in 4000-400 cm^{-1}. Powder X-ray diffraction patterns were tested through Bruker D8 ADV ANCE X-ray powder diffractometer (Cu-Kα, λ = 1.5418 Å) with 2θ at 5-50°. The thermogravimetric analyses were tested on NETZSCH STA 449C microanalyzer (N_2 atmosphere, 10 °C min^{-1}) at 35~800 °C. Gas sorption isotherms were acquired by ASAP 2020 M adsorption equipment.

Synthesis of H_3L. 5-((carboxy-3-ylthio) methyl) isophthalic acid was prepared by mixing 3-mercaptobenzoic acid and 5-(bromomethyl) isophthalic acid in acetone at refluxing temperature for 24 h. After cooling down to room temperature, the white solid of H_3L was collected by filtration with a yield of 88%. IR/cm^{-1} (KBr): 3438 (m),3084 (m), 2972 (w), 2790 (w), 2517 (m), 2148 (w), 2031 (w), 1865 (w), 1672 (s), 1620 (s), 1475 (s), 1348 (m), 1265 (s), 1209 (s), 1105 (s), 974 (m), 912 (m), 860 (w), 812 (s), 771 (s), 687 (s), 611 (m), 484 (w), 426 (m). ^{1}HNMR (400 MHz, DMSO) δ 13.18 (s, 3H), 8.32 (t, J = 1.6 Hz, 1H), 8.13 (d, J = 1.5 Hz, 2H), 7.81 (t, J = 1.6 Hz, 1H), 7.76 - 7.71 (m, 1H), 7.61 - 7.57 (m, 1H), 7.42 (t, J = 7.8 Hz, 1H), 4.45 (s, 2H).

X-ray Crystal Structure Determination. The single crystal X-ray diffractions were tested on Bruker SMART APEX II CCD diffractometer equipped with graphite monochromated Mo-Kα radiation (λ = 0.71073 Å) via ϕ/ω scan method. The diffraction data were corrected for Lorentz and polarization effects for empirical absorption based on multi-scan. The structures were solved by the direct methods and refined on F^2 via *SHELXTL* program. The anisotropic thermal parameters were applied to non-hydrogen atoms. The hydrogen atoms of ligands were calculated and added at ideal positions. The crystallographic data of complex **1** and **2** are summrized in Table 1, and the selected bond lengths and angles are listed in Table S1. The CCDC numbers are 2012400 for **1** and 2044112 for **2**, respectively.

Gas sorption measurements. Before gas sorption,**1** was soaked in dichloromethane (CH_2Cl_2) for three days, then heating the sample under vacuum to get **1a**.

Catalytic Experiment. The catalytic reactions were conducted at the ambient temperature and 0.1 MPa pressure under solvent free environment in a 10 mL Schlenk tube using epoxides (20 mmol) with CO_2 catalyzed by **1a** and a cocatalyst of tetra-ntertbutylammonium bromide (TBAB 2 mmol) under stirring for 6 h (800 rpm). 1H NMR analysis was used to monitor the products and yields of products.

Table S1 Selected bond lengths (Å) and bond angles (º) for **1-2**

Complex 1			
Cu(1)-O(1)	1.9747(19)	O(4)#3-Cu(1)-O(1)	170.65(8)
Cu(1)-O(1)#1	1.9667(18)	O(4)#3-Cu(1)-O(1)#1	93.54(8)
Cu(1)-O(2)	2.2389(19)	O(4)#3-Cu(1)-N(2)	87.74(9)
Cu(1)-O(4)#3	1.917(2)	N(2)-Cu(1)-Cu(1)#1	132.30(7)
Cu(1)-N(2)	2.007(2)	N(2)-Cu(1)-O(2)	95.31(9)
Cu(1)-Cu(1)#1	2.9656(7)	O(1)#1-Cu(2)-O(3)	88.58(8)
Cu(2)-O(1)#1	1.9430(18)	O(1)#1-Cu(2)-O(6)#2	94.32(8)
Cu(2)-O(3)	1.966(2)	O(1)#1-Cu(2)-O(5)#3	95.59(8)
Cu(2)-O(6)#2	1.949(2)	O(1)#1-Cu(2)-N(1)	172.61(10)
Cu(2)-O(5)#3	2.208(2)	O(3)-Cu(2)-O(5)#3	106.92(9)
Cu(2)-N(1)	1.996(2)	O(3)-Cu(2)-N(1)	86.97(9)
O(2)-Cu(1)-Cu(1)#1	96.17(5)	O(6)#2-Cu(2)-O(3)	149.96(9)
O(1)-Cu(1)-Cu(1)#1	41.10(5)	O(6)#2-Cu(2)-O(5)#3	102.55(9)
O(1)#1-Cu(1)-Cu(1)#1	41.30(5)	O(6)#2-Cu(2)-N(1)	86.62(9)
O(1)#1-Cu(1)-O(2)	101.80(7)	N(1)-Cu(2)-O(5)#3	91.35(9)
O(1)-Cu(1)-O(2)	87.58(7)	C(20)-O(6)-Cu(2)#7	128.43(18)
O(1)#1-Cu(1)-O(1)	82.39(8)	C(14)-O(5)-Cu(2)#6	127.22(19)
O(1)#1-Cu(1)-N(2)	162.21(9)	C(22)-N(2)-Cu(1)	122.9(2)
O(1)-Cu(1)-N(2)	93.58(9)	C(26)-N(2)-Cu(1)	119.3(2)
O(4)#3-Cu(1)-Cu(1)#1	134.26(7)	C(2)-N(1)-Cu(2)	122.9(2)
O(4)#3-Cu(1)-O(2)	101.52(8)	C(6)-N(1)-Cu(2)	120.3(2)
C(1)-O(2)-Cu(1)	117.57(17)	Cu(2)#1-O(1)-Cu(1)#1	108.58(9)
Cu(1)#1-O(1)-Cu(1)	97.60(8)	Cu(2)#1-O(1)-Cu(1)	115.77(9)
Cu(1)#1-O(1)-H(1)	118.2	Cu(2)#1-O(1)-H(1)	102.6
Cu(1)-O(1)-H(1)	114.6	C(1)-O(3)-Cu(2)	126.27(19)
C(14)-O(4)-Cu(1)#6	125.03(19)		

Symmetry codes: #1 -x+2, -y+2, -z; #2 x+1, y, z; #3 x, y+1, z; #4 -x+1, -y+3, -z; #5 -x+2, -y+1, -z+1; #6 x, y-1, z; #7 x-1, y, z.

Complex 2			
Mn(1)-O(1)	2.1613(18)	O(1)#1-Mn(1)-O(5)#3	88.11(7)
Mn(1)-O(1)#1	2.1614(18)	O(1)-Mn(1)-O(5)#2	88.11(7)
Mn(1)-O(5)#2	2.2058(17)	O(1)-Mn(1)-O(5)#3	91.89(7)
Mn(1)-O(5)#3	2.2058(17)	O(1)-Mn(1)-O(6)#4	92.94(7)
Mn(1)-O(6)#4	2.1671(16)	O(1)#1-Mn(1)-O(6)#4	87.06(7)
Mn(1)-O(6)#5	2.1671(16)	O(1)-Mn(1)-O(6)#5	87.06(7)
Mn(2)-O(2)#6	2.1204(18)	O(1)#1-Mn(1)-O(6)#5	92.94(7)
Mn(2)-O(3)	2.0989(18)	O(5)#3-Mn(1)-O(5)#2	180.0
Mn(2)-O(4)	2.1756(19)	O(6)#4-Mn(1)-O(5)#2	91.69(7)
Mn(2)-O(6)#7	2.2370(17)	O(6)#5-Mn(1)-O(5)#3	91.69(7)
Mn(2)-O(7)#7	2.482(2)	O(6)#5-Mn(1)-O(5)#2	88.31(7)
Mn(2)-N(2)	2.232(2)	O(6)#4-Mn(1)-O(5)#3	88.31(7)
O(1)-Mn(1)-O(1)#1	180.0	O(6)#4-Mn(1)-O(6)#5	180.00(10)
O(1)#1-Mn(1)-O(5)#2	91.89(7)	O(2)#6-Mn(2)-O(4)	94.63(8)
O(2)#6-Mn(2)-O(6)#7	108.14(7)	O(3)-Mn(2)-N(2)	86.24(8)
O(2)#6-Mn(2)-O(7)#7	162.91(7)	O(4)-Mn(2)-O(6)#7	86.34(7)
O(2)#6-Mn(2)-N(2)	115.34(8)	O(4)-Mn(2)-O(7)#7	84.51(8)
O(3)-Mn(2)-O(2)#6	89.39(8)	O(4)-Mn(2)-N(2)	87.45(8)
O(3)-Mn(2)-O(4)	173.52(7)	O(6)#7-Mn(2)-O(7)#7	54.78(6)
O(3)-Mn(2)-O(6)#7	97.25(7)	N(2)-Mn(2)-O(6)#7	136.42(8)
O(3)-Mn(2)-O(7)#7	93.14(8)	N(2)-Mn(2)-O(7)#7	81.70(8)

Symmetry codes: #1 -x+3/2, -y+1/2, -z+2; #2 -x+3/2, -y+1/2, -z+1;#3 x, y, z+1; #4 x, -y+1, z+1/2; #5 -x+3/2, y-1/2, -z+3/2; #6 x, y ,z-1; #7 -x+3/2, y-1/2, -z+1/2; #8 -x+1, y, -z+1/2; #9 -x+3/2, y+1/2, -z+3/2; #10 -x+3/2, y+1/2, -z+1/2.

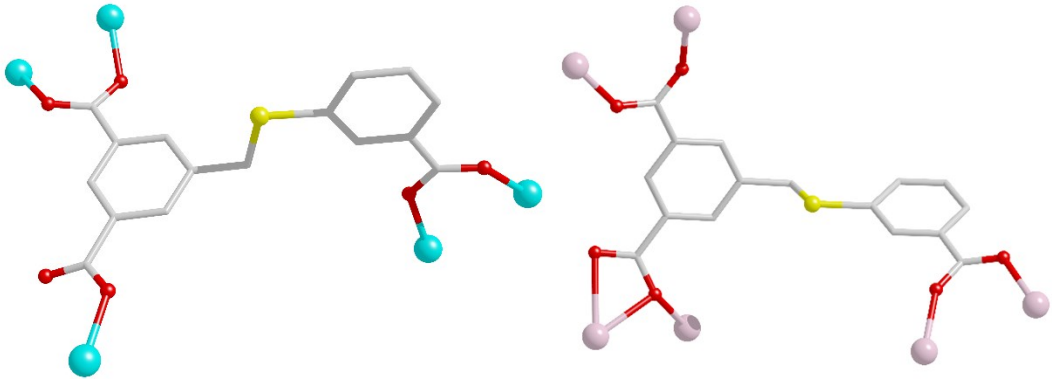

(a) **(b)**

Fig. S1 Coordination mode of L^{3-} in **1**-**2**.

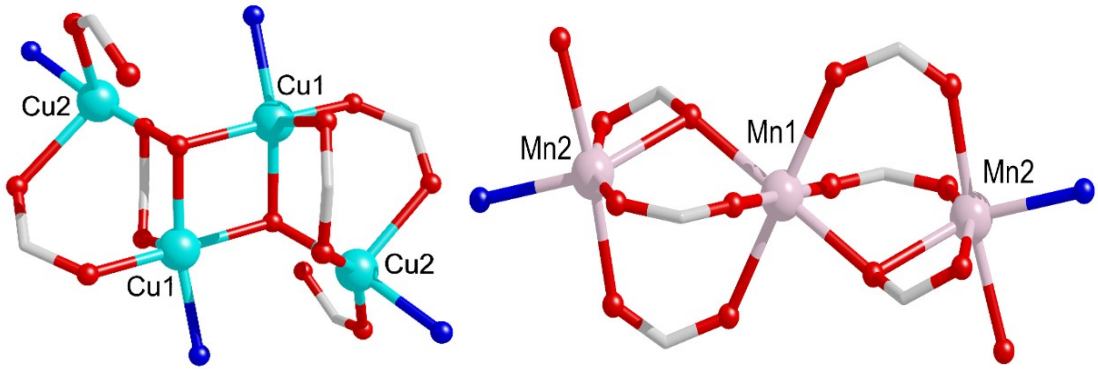

(a) **(b)**

Fig. S2 (a) The tetranuclear cluster in **1**. (b) The trinuclear cluster in **2**.

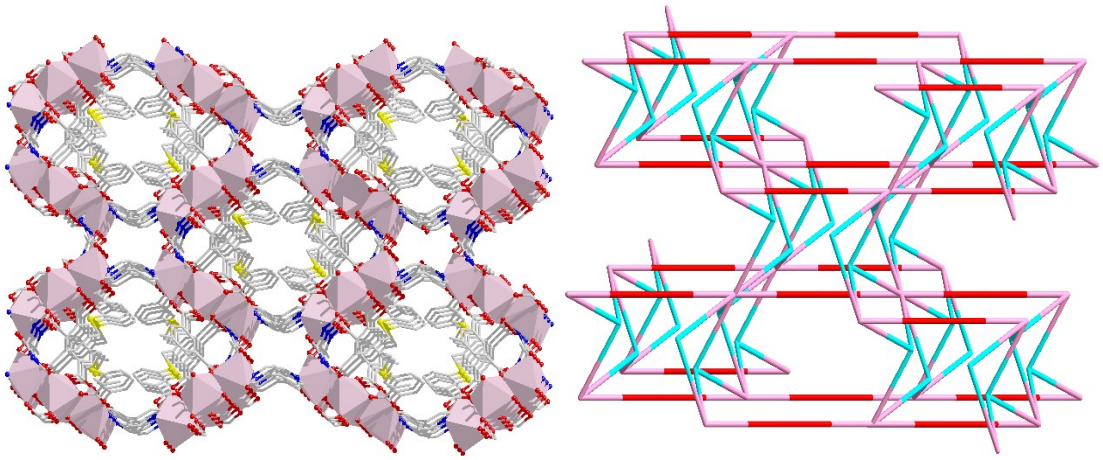

(a) **(b)**

Fig. S3 (a) The 3D porous framework of **2**. (b) Topological net of **2**.

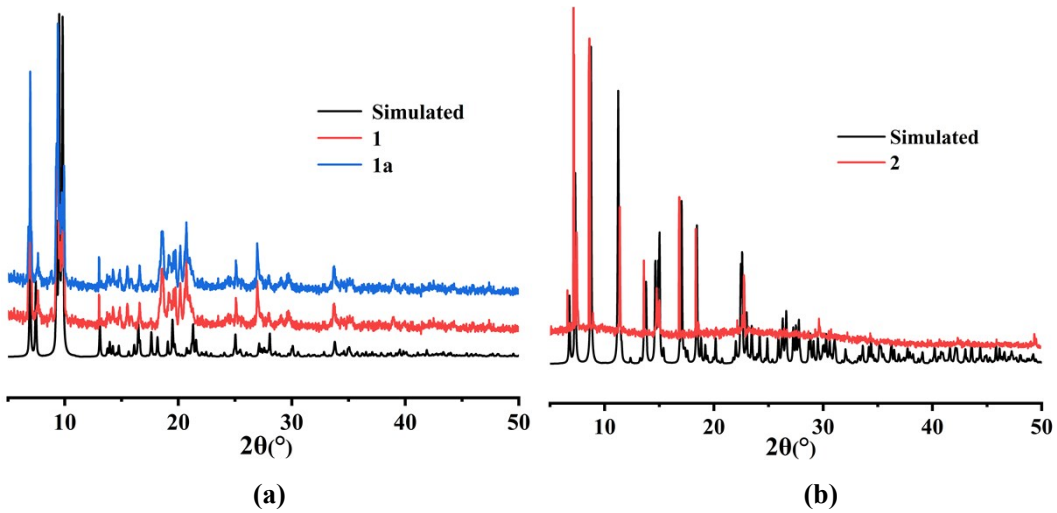

Fig. S4 The PXRD patterns of the as-synthesized products **1** (a) and **2** (b).

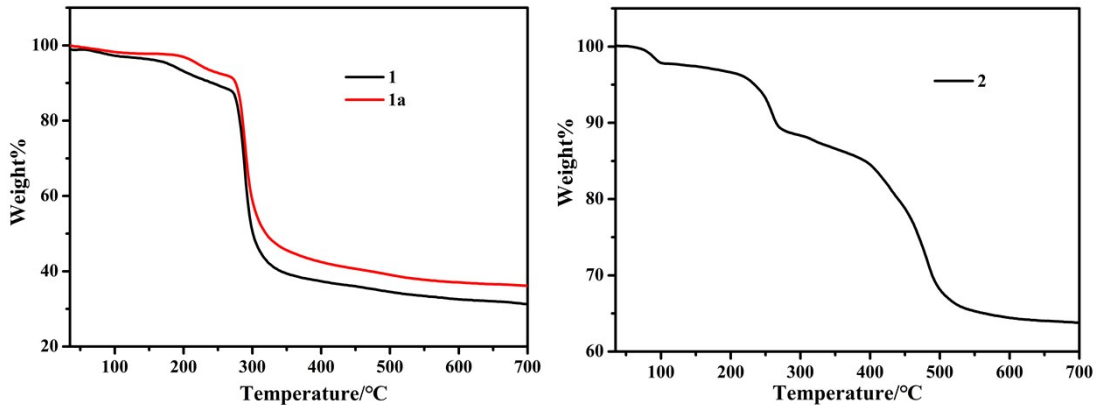

Fig. S5 The TGA curves for **1** and **2**.

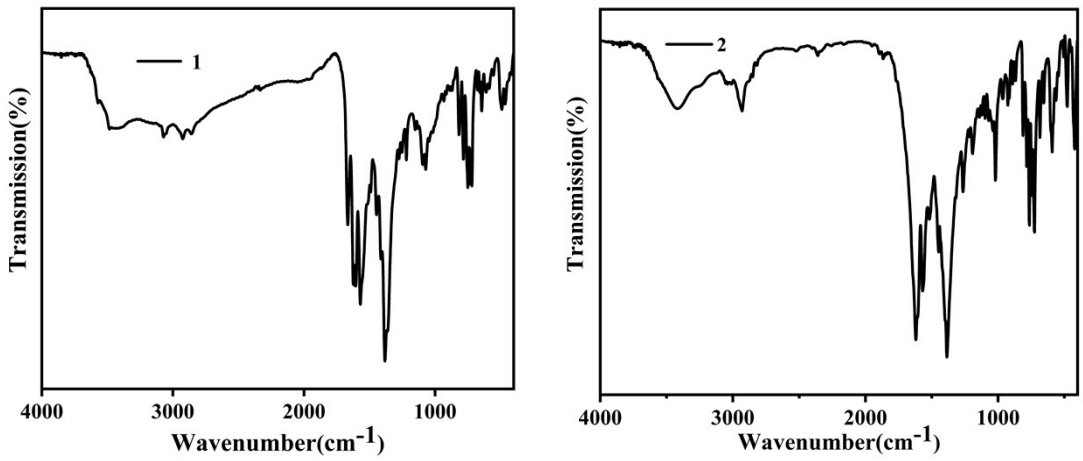

Fig. S6 FT-IR spectras for **1** and **2**.

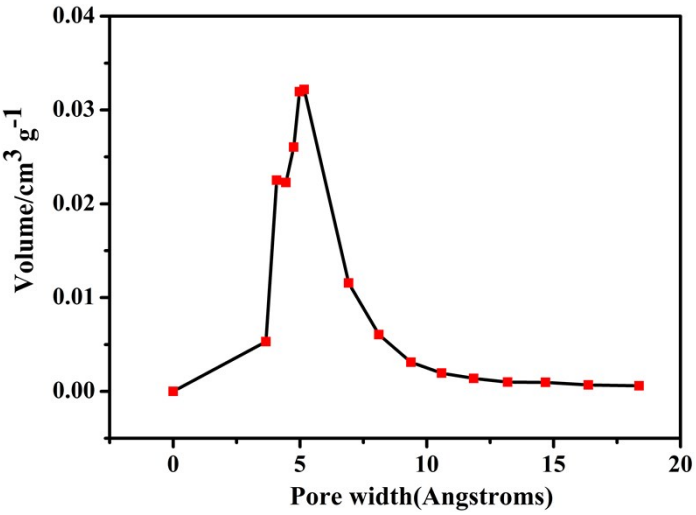

Fig. S7 PSD obtained from the 195 K isotherms using H-W mode of **1a**.

IAST adsorption selectivity calculation

The experimental isotherm data for pure CO_2 and CH_4 (measured at 273 K and 298 K) were fitted using a Langmuir-Freundlich (L-F) model.

$$q = \frac{a * b * p^{c}}{1 + b * p^{c}}$$

Where q and p are adsorbed amounts and pressures of component i, respectively. The adsorption selectivity for binary mixtures of CO_2/CH_4 at 273 K and 298 K, defined by

$$S_{ads} = (q_1/q_2)/(p_1/p_2)$$

Where qi is the amount of i adsorbed and pi is the partial pressure of i in the mixture.

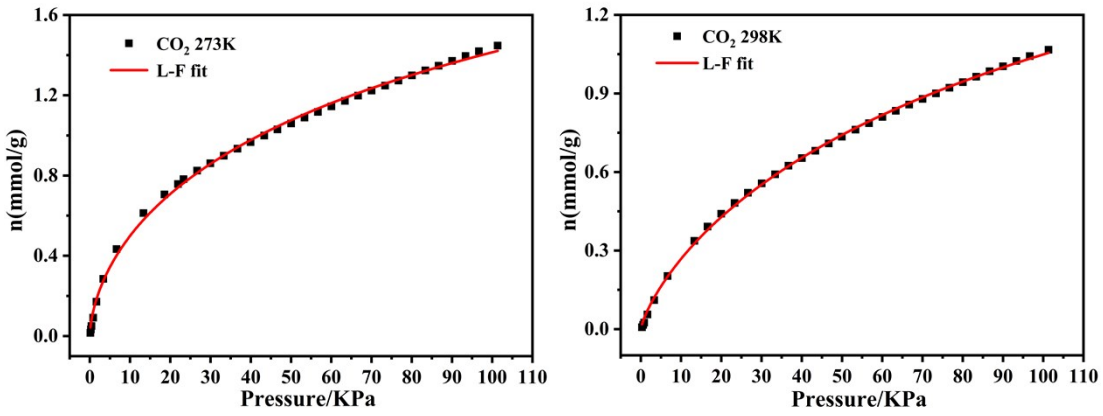

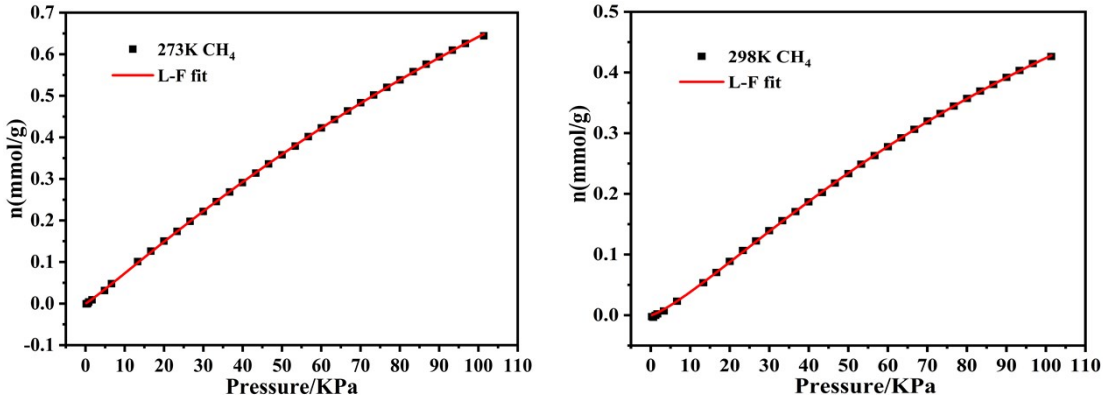

Fig. S8 CO_2 adsorption isotherms of **1a** at 273K with fitting by L-F model: a= 3.51934, b= 0.04067, c = 0.60904, Chi^2 = 3.72175E-4, R^2 = 0.99823; CO_2 adsorption isotherms of **1a** at 298K with fitting by L-F model: a =2.46738, b = 0.02008, c = 0.78313, Chi^2 = 8.0536E-5, R^2 = 0.99932; CH_4 adsorption isotherms of **1a** at 273K with fitting by L-F model: a = 2.17203, b = 0.00287, c = 1.08228, Chi^2 = 3.08297E-6, R^2 = 0.99994; CH_4 adsorption isotherms of **1a** at 298K with fitting by L-F model: a = 0.99848, b = 0.00217, c = 1.26605, Chi^2 = 2.49806E-6, R^2 = 0.99988.

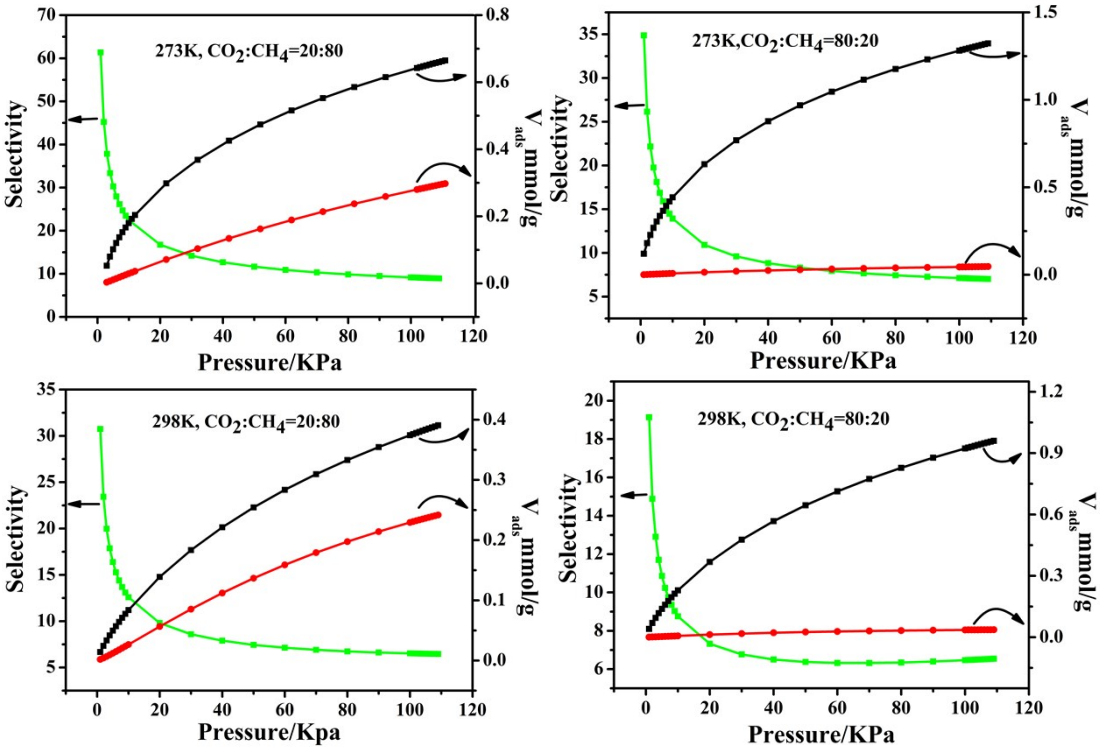

Fig. S9 IAST adsorption selectivity of **1a** for equimolar mixtures of CO_2 and CH_4 at 273 K and 298 K.

Calculation of sorption heat for CO_2 uptake using Virial 2 model

$$\ln P = \ln N + 1/T \sum_{i=0}^{m} aiN^i + \sum_{i=0}^{n} biN^i \qquad Q_{st} = -R\sum_{i=0}^{m} aiN^i$$

The above equation was applied to fit the combined CO_2 isotherm data for desolvated **1a** at 273 K

and 298 K, where *P* is the pressure, *N* is the adsorbed amount, *T* is the temperature, ai and bi are virial coefficients, and m and n are the number of coefficients used to describe the isotherms. Q_{st} is the coverage-dependent enthalpy of adsorption and *R* is the universal gas constant.

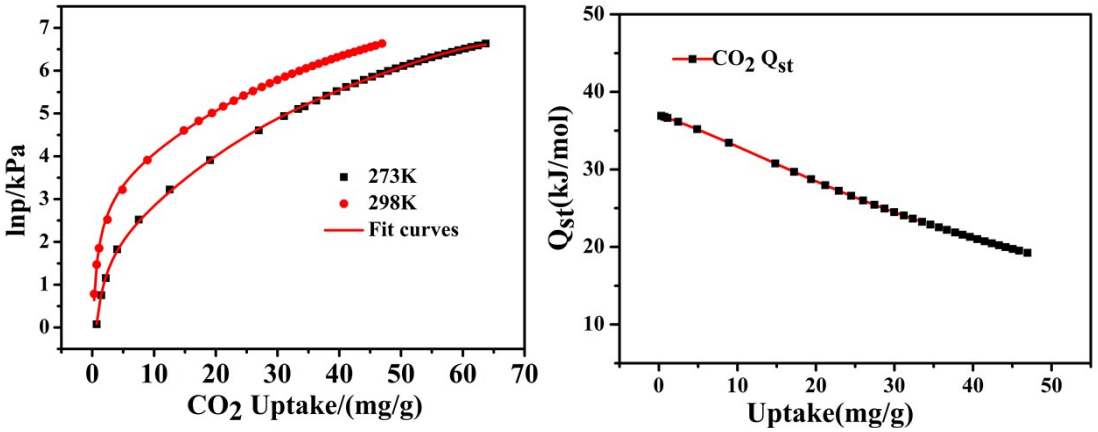

(a) **(b)**

Fig. S10 (a) CO_2 adsorption isotherms for **1a** with fitting by Virial 2 model. Fitting results: a0 = -4451.39526, a1 = 39.49374, a2 = 1.38865, a3 = -0.05355, a4 =7.62549E-4, a5 = -4.11817E-6; b0 = -11.32327, b1 = 0.00254, Chi^2 = 0.00451, R^2 = 0.99966. (b) Isosteric heat of CO_2 adsorption for **1a** estimated by the virial equation from the adsorption isotherms 298 K.

Table S2 Comparison of CO_2 separation performances at 298 K of·**1a** and other MOFs.

MOF	Selectivity	Ref.
$[Cu_{0.5}(bpdado)_{0.5}(bpe)_{0.5}]\cdot 3H_2O\}_n$	15.5	1
$[H_2N(CH_3)_2]_2[Cu(L)]$	30.8	2
$Cu_2(pbpta)$	6	3
Cu-TDPDA	13.8	4
$[Cu(bpy)_2(SiF_6)]$	10.5	5
TIFSIX-1-Cu	11	6
$(Cu_4I_4)[Cu_2\text{-}PDC_2(H_2O)_2]$	8	7
[Cu(INIA)]	4.3	8
$\{[Cu_2(L)(4,4'\text{-bipy})(OH)]\cdot H_2O\}_n$	**22.5**	**This work**

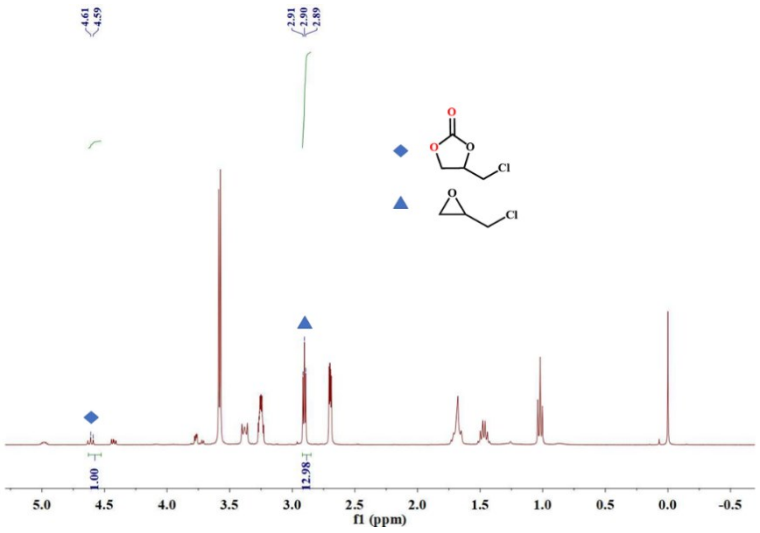

(a) [1]H NMR spectrum of cyclic carbonate and epoxide with complex **1a** and TBAB (Table 2, entry 1).

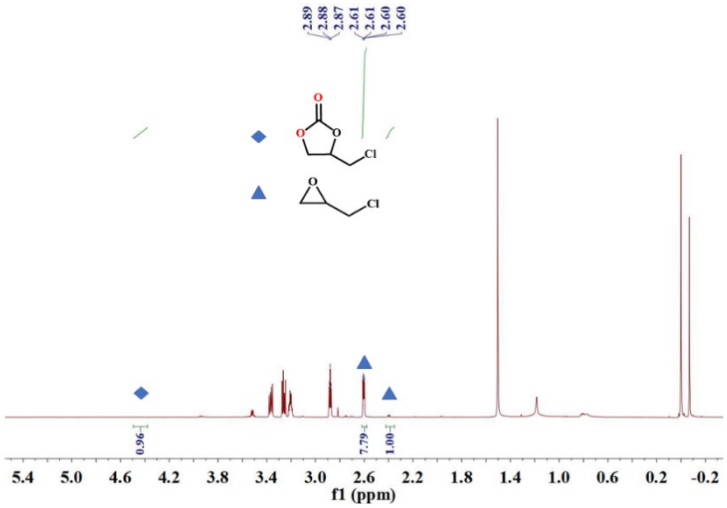

(b) [1]H NMR spectrum of cyclic carbonate and epoxide with complex **1a** and TBAB (Table 2, entry 2).

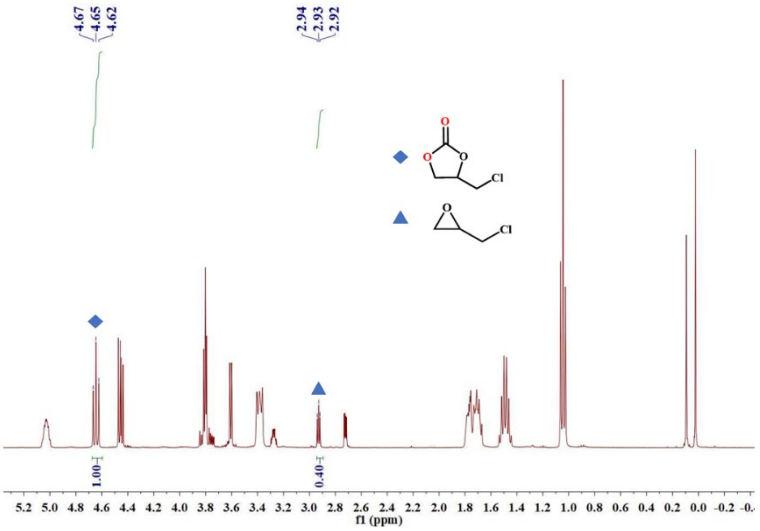

(c) [1]H NMR spectrum of cyclic carbonate and epoxide with complex **1a** and TBAB (Table 2, entry 3).

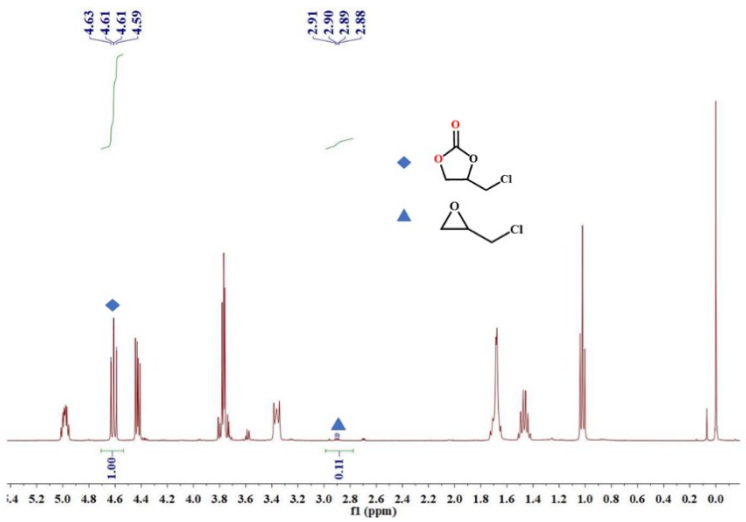

(d) ^{1}H NMR spectrum of cyclic carbonate and epoxide with complex **1a** and TBAB (Table 2, entry 4).

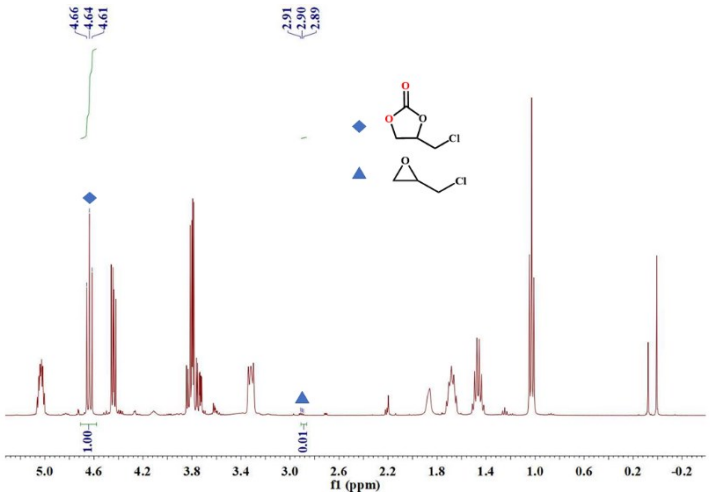

(e) ^{1}H NMR spectrum of cyclic carbonate and epoxide with complex **1a** and TBAB (Table 2, entry 5).

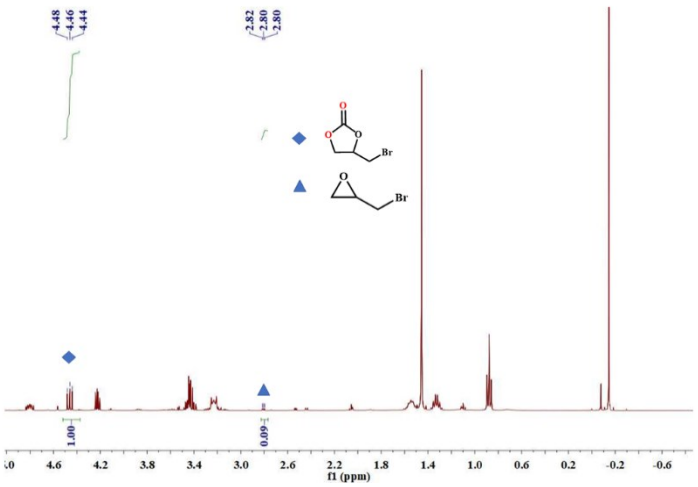

(f) ^{1}H NMR spectrum of cyclic carbonate and epoxide with complex **1a** and TBAB (Table 2, entry 6).

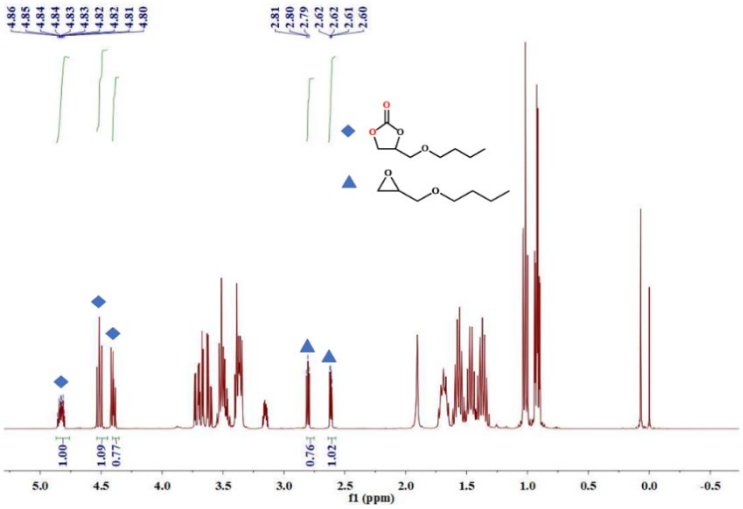

(g) [1]H NMR spectrum of cyclic carbonate and epoxide with complex **1a** and TBAB (Table 2, entry 7).

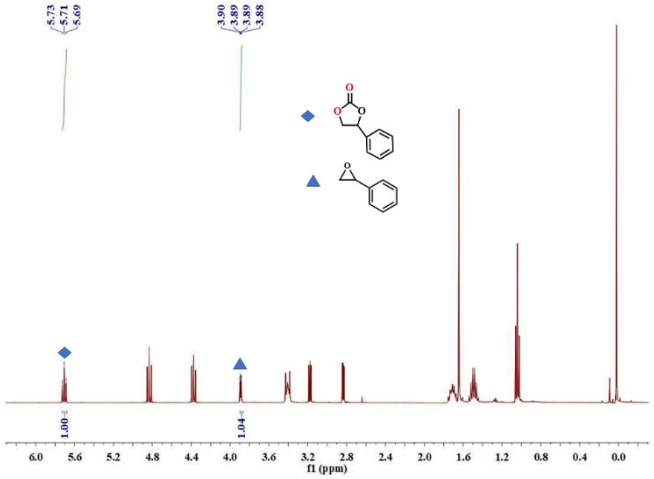

(h) [1]H NMR spectrum of cyclic carbonate and epoxide with complex **1a** and TBAB (Table 2, entry 8).

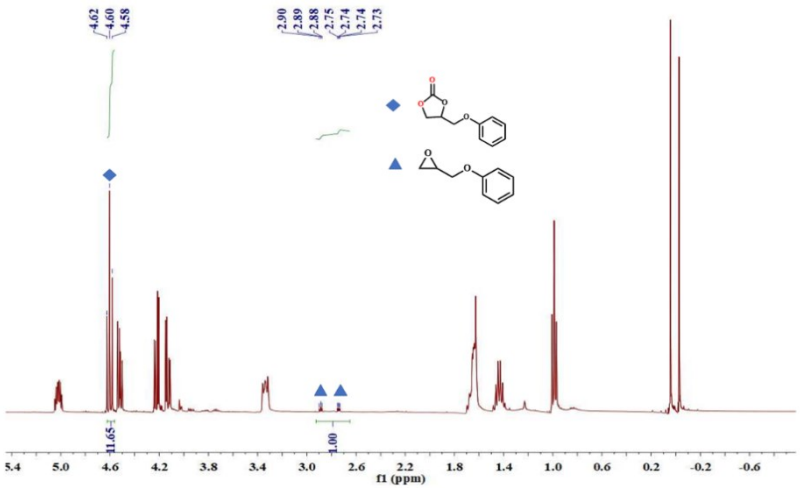

(i) [1]H NMR spectrum of cyclic carbonate and epoxide with complex **1a** and TBAB (Table 2, entry 9).

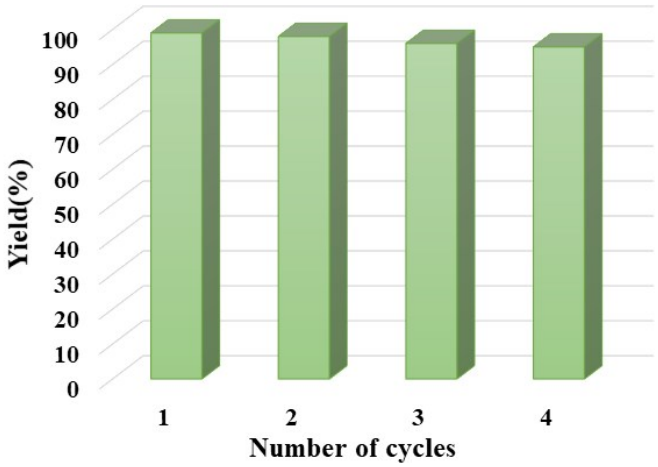

Fig. S11 Cyclic experiment on the cycloaddition reaction of CO_2 and epichlorohydrin.

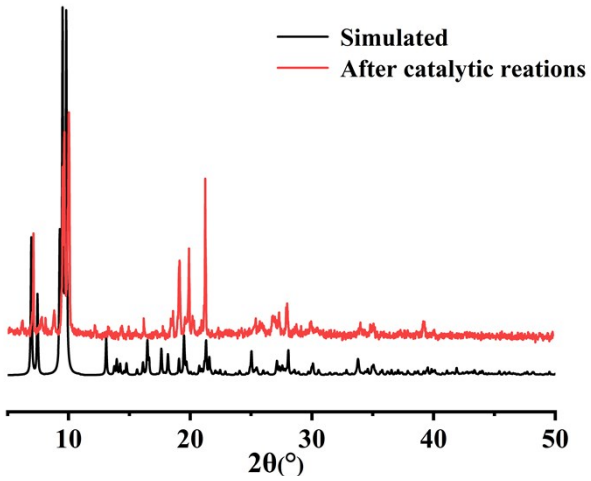

Fig. S12 PXRD patterns of **1a** after four runs catalytic reactions.

References

1 W. Q. Zhang, R. D. Wang, Z. B. Wu, Y. F. Kang, Y. P. Fan, X. Q. Liang, P. Liu and Y. Y. Wang, *Inorg. Chem.*, 2018, **57**, 1455-1463.

2 B. Liu, H. F. Zhou, L. Hou, Z. Zhu and Y. Y. Wang, *Inorg. Chem. Front.*, 2016, **3**, 1326-1331.

3 G. Verma, S. Kumar, T. Pham, Z. Niu, L. Wojtas, J. A. Perman and S. Ma, *Cryst. Growth Des.*, 2017, **17**, 2711-2717.

4 Z. Zhang, Z. Li and J. Li, *Langmuir,* 2012, **28**, 12122-12133.

5 S. D. Burd, S. Ma, J. A. Perman, B. J. Sikora, R. Q. Snurr, P. K. Thallapally, J. Tian, L. Wojtas and M. J. Zaworotko, *J.Am. Chem. Soc.*, 2012, **134**, 3663-3666.

6 P. Nugent, V. Rhodus, T. Pham, B. Tudor, K. Forrest, L. Wojtas, B. Space and M. Zaworotko, *Chem. Commun.*, 2013, **49**, 1606-1608.

7 H. He, F. Sun, S. Ma and G. Zhu, *Inorg.Chem.*, 2016, **55**, 9071-9076.

8 Y. Xiong, Y. Z. Fan, R. Yang, S. Chen, M. Pan, J. J. Jiang and C. Y. Su, *Chem. Commun.*, 2014, **50**, 14631-14634.